Inhomogeneous broadening and the Kosterlitz-Thouless transition

M. Collins, G. Agnolet, W. M. Saslow, and E. Krotscheck
Physics Department, Texas A&M University, College Station, Texas 77843
(Received 19 May 1992; revised manuscript received 20 October 1992)

Torsional-oscillator studies of very thin ^{4}He films have found nonuniversal behavior of the superfluid response as a function of coverage. The temperature width of the superfluid transition region is nonmonotonic in the areal density n and exhibits cusplike variations at half of the layering period. We explore the assumption that this additional broadening is caused by macroscopic inhomogeneities in the substrate potential; such a theory for inhomogeneous broadening can be constructed from the Kosterlitz-Nelson relation between the superfluid areal density n_s and the transition temperature T_c by determining the theoretical "sensitivity" S of n_s to variations in the strength of the substrate potential. For substrate models that are atomically uniform, a simple microscopic hypernetted-chain calculation (without either "elementary diagrams" or three-body correlations, but with an optimized Jastrow function) finds this sensitivity always to be of the same sign, and yields reasonable order-of-magnitude agreement with experiment. However, models for which the sensitivity does not change sign appear to be incapable of yielding either the cusps or the half-periodicity of the data. We suggest that these properties may occur with a more recently developed (and more sophisticated) version of hypernetted-chain theory, wherein "elementary diagrams" and three-body correlations are incorporated.

I. INTRODUCTION

Although many theories[1] predict that long-range order does not occur in two-dimensional systems with a continuous symmetry group, thin films of liquid ^{4}He are well known to exhibit superfluid behavior below some critical temperature T_c. Kosterlitz and Thouless[2] (KT) showed that for such systems a form of topological or quasi-long-range order can exist at low temperatures and that the thermal excitations responsible for the disappearance of superfluidity at high temperatures are quantized vortices. An important prediction of this theory[3] is that the superfluid density at T_c exhibits universal scaling. In particular, the superfluid areal density $n_s(T)$ obeys a universal scaling relation of the form

$$\lim_{T\to T_c^-} \frac{n_s(T)}{T} = \frac{n_s(T_c^-)}{T_c} = \frac{2mk_B}{\pi\hbar^2}, \tag{1}$$

where m is the atomic mass of ^{4}He.

To compare the predictions of the KT theory with physical measurements, one must take into account the time dependent flow velocities that are normally present in the experiments. In torsional oscillator experiments,[4–6] the helium film is adsorbed on substrates with large surface areas that are mounted to a torsional element. At high temperatures, the helium film is viscously clamped to the substrate and therefore contributes its entire moment of inertia to the resonant frequency of the oscillator. Below the superfluid transition, as $n_s(T)$ grows, the resonant frequency of the oscillator increases as the fraction of the helium that decouples from the motion of the substrate increases. Furthermore, in addition to the intrinsic mechanical damping Q_0^{-1} of the torsional oscillator, one observes a damping associated with the relative motion of the substrate and the superfluid fraction. In the analysis of vortex dynamics by Ambegaokar, Halperin, Nelson, and Siggia[7] (AHNS), the response of the helium film to the velocity field induced by the substrate motion involves a characteristic diffusion constant D for the vortices in the film. A direct consequence of this analysis is that, because of the finite frequency ω of the oscillator employed in the measurement, the superfluid transition is broadened: the apparent superfluid density does not vanish immediately above T_c as in the KT theory, but smoothly decreases to zero as the temperature is increased above T_c. In this same temperature region, the additional dissipation is strongly peaked, falling rapidly to zero at both high and low temperatures. Overall, there is good quantitative agreement between the AHNS predictions, for the temperature dependence of both the superfluid density and the dissipation, and the experimental data[4–6] on helium films with transition temperatures above 1 K.

A more ambitious test of the AHNS theory can be made by comparing the superfluid response for films of different coverages. By making a few additional assumptions[6] within the AHNS theory, it is straightforward to show that the dynamical response of the film should also obey a universal scaling relationship in the region of T_c. Specifically, the superfluid density and dissipation, when normalized by T_c, should be universal functions of the reduced temperature, T/T_c. Consequently, when analyzed in this fashion, the superfluid density and the dissipation from films of different superfluid coverages should each collapse onto a single curve.

A dramatic departure from this predicted scaling behavior is observed[6] for helium films adsorbed on a Mylar[8] substrate that have transition temperatures less than 1 K, corresponding to coverages of less than 1 atomic layer of superfluid at $T = 0$. The discrepancy is observed in the

coverage dependence of both the reduced superfluid density and the reduced dissipation, but is most clearly seen in the behavior of the dissipation peaks. As a function of coverage, most of the scaled dissipation peaks are consistent with the scaling prediction in that they have similar shapes, but at a few special coverages the scaled dissipation peaks are significantly narrower. Moreover, it is the narrower dissipation peaks rather than the broader dissipation peaks that are consistent with the theoretically predicted temperature dependence.

A clue to understanding this unusual behavior can be found by examining the integrated area of the dissipation peaks. Although the dissipation peaks have different shapes, the area under each peak does approximately scale with T_c, as expected from the scaling prediction. We thus hypothesize that there exists a mechanism that preserves the scaling behavior of the area under the peaks, and broadens the superfluid transition at most coverages, but is ineffective at certain coverages. One such mechanism is inhomogeneous broadening caused by spatial variation of T_c due to macroscopic inhomogeneities in n_s that are induced by spatial variations of the substrate interaction potential.

For simplicity, we assume that the macroscopic inhomogeneity, or roughness, of the substrate, is characterized by R_s, its spatial scale, and by $\Delta\lambda$, a dimensionless measure of its amplitude ($\Delta\lambda = 0$ for a perfectly uniform potential). If R_s is large in comparison with the dynamic length scale $r_D = \sqrt{14D/\omega}$ (Refs. 7 and 9) probed by the experiment, then one can expect n_s and, by Eq. (1), T_c, to be inhomogeneous. (If R_s is very small compared to r_D, then the system will appear to be uniform.) Thus, for $R_s \gg r_D$, in addition to the homogeneous broadening associated with the vortex dynamics,[7] there should also be an inhomogeneous broadening in the width of the transition region, due to the dependence of n_s on the local strength of the substrate potential. For a typical experiment at 1300 Hz, we expect that $r_D \approx 300\, r_0$, where r_0, the vortex core radius, is on the order of atomic dimensions (4 Å). For comparison, Mylar contains small bubbles and imperfections, the smallest bubbles having diameters less than 2.5 μm with average separation of 12 μm, and larger bubbles having diameters of about 8 μm and average separation of 150 μm; there can also be flakes as large as 50–100 μm on the surface.[6] Thus it is not unreasonable to expect macroscopic inhomogeneities to occur on a scale larger than 1000 Å.

In this work, we reanalyze existing torsional oscillator data[10,11] to estimate the additional contribution to the broadening of the transition due to inhomogeneities in the substrate. We then employ a simple model for which the inhomogeneous broadening can be calculated from the sensitivity of n_s to inhomogeneities in the substrate potential. Using a simple microscopic hypernetted-chain (HNC) theory for an atomically uniform substrate (i.e., the substrate potential depends only on the distance z from the substrate) we calculate this sensitivity and show that, for $\Delta\lambda \approx 0.005$, it leads to good order-of-magnitude agreement with the data. However, it does not explain the cusplike behavior nor the half-periodicity of the data. It is possible that recent developments using a more sophisticated HNC theory will be capable of explaining the data.

II. EXTRACTION OF INHOMOGENEOUS BROADENING FROM DATA

To simplify the following analysis we choose the full width at half maximum of the dissipation peaks to be the measure of the characteristic temperature width of the superfluid transition, ΔT. We assume that the experimental width, $\Delta T^{\rm expt}$, has two contributions: a homogeneous coverage-independent contribution, $\Delta T_h^{\rm th}$, computed as in Refs. 7 and 9, and an inhomogeneous coverage-dependent contribution, $\Delta T_{\rm inh}^{\rm expt}$, caused by macroscopic inhomogeneities in the areal density at fixed chemical potential:

$$(\Delta T^{\rm expt})^2 = (\Delta T_h^{\rm th})^2 + (\Delta T_{\rm inh}^{\rm expt})^2. \tag{2}$$

If the broadening mechanism preserves the universal scaling, then the area under the dissipation curve should not change from its value without inhomogeneous broadening. As a consequence, a knowledge of H_h, defined as the value of the maximum dissipation $(Q^{-1} - Q_0^{-1})_{\rm max}$ for the homogeneous case, yields $\Delta T_h^{\rm th}$ via the relation

$$\Delta T_h^{\rm th} H_h (1-\chi) \approx \Delta T^{\rm expt} H^{\rm expt}, \tag{3}$$

where $(1-\chi)$ is the fraction of the superfluid that is free to decouple from the motion of the substrate and contribute to the dissipation.[6] Substitution into Eq. (2) yields the dimensionless width

$$\frac{\Delta T_{\rm inh}^{\rm expt}}{T_P} = \frac{\Delta T^{\rm expt}}{T_P}\left[1 - \left(\frac{H^{\rm expt}}{H_h(1-\chi)}\right)^2\right]^{1/2}, \tag{4}$$

where T_P is the temperature where the dissipation peak of the transition reaches its maximum. Formally one should use T_c, but T_P is more easily identified from the experimental data than T_c and is not significantly different from T_c. In the above equation, all but H_h can be determined from experiment. To obtain H_h, we employ[9]

$$H_h = \frac{Am}{\pi M} n_0(T_c)\tilde{\epsilon}^{-1}(T_P), \tag{5}$$

where A is the area of the film, M is the total mass of the oscillator, n_0 is the superfluid areal density due to nonvortex excitations, and $\tilde{\epsilon}$ is the "dielectric constant" due to the polarization caused by bound pairs of vortices in the static limit of zero oscillator frequency. This assumes that n_0 varies only slightly in the temperature range of the dissipation peak, which permits an analogy between vortices in the superfluid and the neutral two-dimensional Coulomb gas.[9] Since $\tilde{\epsilon}$ is well behaved throughout the phase transition, in Eq. (5) we take

$$\tilde{\epsilon}(T_P) \approx \tilde{\epsilon}(T_c) \tag{6}$$

and employ[9]

$$\tilde{\epsilon}^{-1}(T_c^-) = \lim_{T \to T_c^-} \frac{n_s(T)}{n_0(T)}, \tag{7}$$

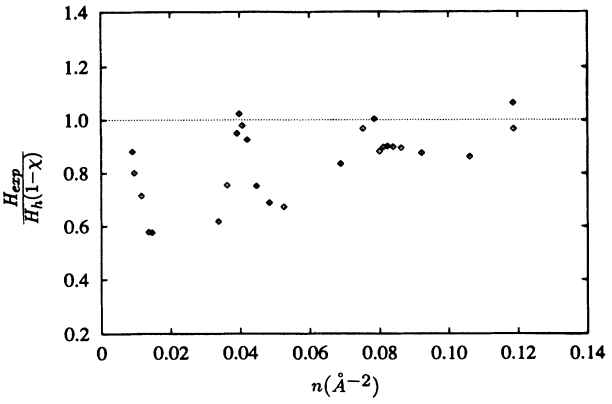

FIG. 1. $H_{\text{expt}}/H_h(1-\chi)$ vs n, where n is the active coverage.

which, with Eq. (1), leads to

$$H_h \approx \frac{2Am^2k_B}{M\pi^2\hbar^2}T_P. \tag{8}$$

In order to check that this approximation for H_h is reasonable, we compute $H^{\text{expt}}/H_h(1-\chi)$ to verify that it is less than unity at all coverages. The data on H^{expt} and ΔT^{expt} are taken from Refs. 10 and 11, and the value $\chi = 0.144$ is taken from Ref. 6. Both of these works employed a Mylar substrate, with an inert coverage of 1.6 atomic layers. The horizontal scale in Fig. 1 considers n to include only the active coverage. One layer corresponds to a coverage of 0.078 Å^{-2}, which is given by the product of the layer thickness [3.6 Å $= (m/\rho)^{1/3}$, where ρ is the mass density of the bulk fluid] and the bulk number density ρ/m.

Figure 1 shows that at certain coverages the experimental height is slightly greater than the χ-modified theoretical height. In the vicinity of these points the variation is very rapid, which we consider to be more like what occurs at a cusp rather than what occurs at a smooth peak. Consequently, we set $H^{\text{expt}} \equiv H_h(1-\chi)$ at these points, thus assuming that there is essentially no inhomogeneous broadening at these coverages and enforcing the cusplike interpretation of the data. Then, with Eq. (8), Eq. (4) can be evaluated, yielding Fig. 2, the "experimental" inhomogeneous width. Figure 2 shows that the inhomogeneous width has half-layer periodicity (about 0.039 Å^{-2}) rather than the full-layer periodicity of 0.078 Å^{-2}. In addition, the reanalyzed data show even more pronounced cusplike behavior at the minima than do the original data.

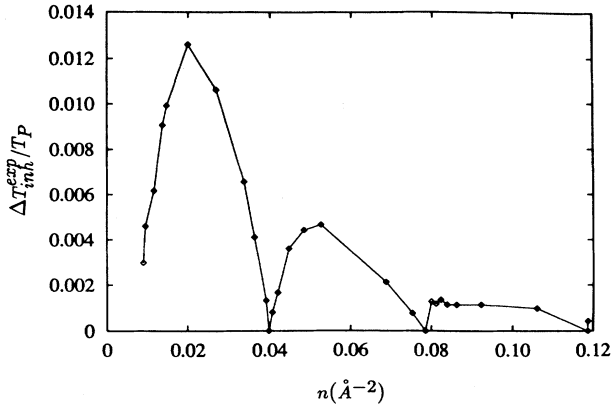

FIG. 2. $\Delta T_{\text{inh}}^{\text{expt}}/T_P = S^{\text{expt}}\Delta\lambda$ vs n, where n is the active coverage.

III. INHOMOGENEOUS BROADENING AND THE "SENSITIVITY" S

To obtain the inhomogeneous broadening $\Delta T_{\text{inh}}^{\text{th}}$, we note that different regions of the substrate are characterized by a common value of the chemical potential μ, despite the variation in the substrate potential. Then, by Eq. (1) we have

$$\Delta T_{\text{inh}}^{\text{th}}/T_P = (\Delta\lambda)S, \tag{9}$$

where we define the "sensitivity"

$$S = -\frac{1}{n_s}\frac{\partial n_s}{\partial\lambda}\bigg|_{\mu} \tag{10}$$

of n_s to dimensionless variations $\Delta\lambda$ in the strength of the substrate potential. (The sign convention is taken so that, in the hypernetted-chain calculations to follow, S is positive; the widths $\Delta T_{\text{inh}}^{\text{th}}$ and $\Delta\lambda$ are necessarily positive.)

IV. INHOMOGENEOUS BROADENING FOR ATOMICALLY UNIFORM SUBSTRATES

In practice, we assume that

$$\frac{\delta n_s}{n_s}\bigg|_{T_c^-} \approx \frac{\delta n}{n}\bigg|_{T=0}, \tag{11}$$

and thus we determine S by rewriting Eq. (10) as

$$S = \frac{1}{n}\frac{(\partial\mu/\partial\lambda)|_n}{(\partial\mu/\partial n)|_{\lambda=1}}, \tag{12}$$

and computing each of the partial derivatives from ground-state properties determined by solving the hypernetted-chain–Euler-Lagrange equations[12] (HNC-EL) for the $T = 0$ ground-state structure of the film. The theory starts from a Jastrow-Feenberg variational ansatz for the many-body wave function of the form

$$\Psi_0(\mathbf{r}_1,\ldots,\mathbf{r}_N) = \exp\frac{1}{2}\left[\sum_i u_1(\mathbf{r}_i) + \sum_{i<j} u_2(\mathbf{r}_i,\mathbf{r}_j) + \ldots\right] \tag{13}$$

and determines the one-body and two-body correlation functions $u_1(\mathbf{r}_i)$ and $u_2(\mathbf{r}_i,\mathbf{r}_j)$ by minimization of the ground-state energy,

$$\frac{\delta}{\delta u_n}\frac{(\Psi_0|H|\Psi_0)}{(\Psi_0|\Psi_0)}(\mathbf{r}_1,\ldots,\mathbf{r}_n) = 0 \qquad (n=1,2). \tag{14}$$

The theory leads to a hierarchy of equations—the HNC equations—which, by inclusion of consecutively more complicated "elementary diagrams," permits a more accurate evaluation of the pair distribution function and of the ground-state energy. In the present work, the Jastrow function $u_1(\mathbf{r}_i)$ is not fixed, but rather is optimized, but we have employed what is otherwise the simplest version of the theory, the so-called "HNC approximation," wherein all "elementary diagrams" are omitted. The most significant (and desirable) contrast to pure density functional theory, which utilizes only the one-body density $n(\mathbf{r})$, is that, as the areal density increases, the one-body density displays a marked layering effect. This feature, which is due to competition between the correlated hard-core repulsion among individual ^{4}He atoms and their attraction to the substrate, is already present in the simplest implementation of the HNC-EL theory used here. To determine S, the denominator is calculated numerically by fixing λ, varying n, and finding the associated variation in μ. The numerator is calculated by fixing n, varying λ ($\lambda = 1$ is the background value), and finding the associated variation in μ.

We have calculated S for models of hydrogen and graphite substrates that are atomically uniform. The model for the hydrogen substrate consists of a 10 Å film of solid H_2 adsorbed on a glass substrate, using the substrate potential $V_H(z)$ suggested by Dupont-Roc,[13]

$$V_H(z) = -9.32\left(\frac{s}{z}\right)^3 - 24.8\left(\frac{s}{z}\right)^5 + 8.86\left(\frac{s}{z}\right)^9 - 19.6\left(\frac{s}{z+10}\right)^3. \quad (15)$$

$V_H(z)$ is given in K, the coordinate normal to the substrate, z, is given in Å, and $s = 3.6$ Å. The potential for graphite, $V_G(z)$, takes the form[14]

$$V_G(z) = e\left[\frac{1}{15}\left(\frac{s}{z}\right)^9 - \frac{1}{2}\left(\frac{s}{z}\right)^3\right], \quad (16)$$

where $e = 48$ K and s is unchanged, giving a van der Waals coefficient of 2240 K Å^3. The above potential has a minimum at $z = 2.75$ Å, whose value is about a factor of 2.5 less than the expected value for an actual graphite substrate; this is necessary to keep the HNC-EL equations from having a local instability due to solid formation.[12]

In order to numerically calculate $\partial\mu/\partial\lambda$ for the given potentials, the HNC-EL equations were first solved for $\lambda = 1$ with different number densities n as input, to obtain $\mu(n)$ and consequently to evaluate $(\partial\mu/\partial n)|_{\lambda=1}$. The calculation was then repeated for fixed values of n with different values of λ: the hydrogen potential was scaled down by a factor of 0.06 to $0.94V_H(z)$, whereas the graphite potential was scaled up to $1.06V_G(z)$. This yielded $(\Delta\mu)_n$, from which $(\partial\mu/\partial\lambda)|_n$ was evaluated.

In Ref. 6, the experimental substrate, Mylar, has a van der Waals coefficient of 2420 K Å^3, and an inert coverage of 1.6 atomic layers. The effective substrate of the Mylar with an overlayer of inert helium should have a van der Waals coefficient similar to the graphite model but with a weaker well depth.

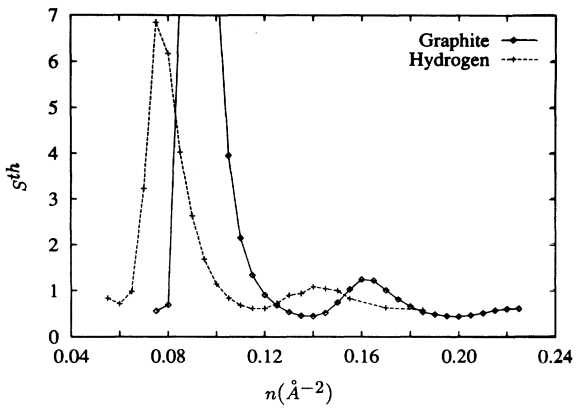

FIG. 3. S^{th} vs n, modeled with graphite and hydrogen substrates.

Figure 3 shows that peaks in the sensitivity occur every time that a new layer starts to form; this occurs roughly every 0.065 Å^{-2}, and is to be compared with 0.078 Å^{-2} of Sec. II. Note that the first peak in both curves of Fig. 3 corresponds to the start of the second layer. We will associate this layer with the first active layer of the experimental substrate. Comparison of both of these figures to Fig. 2 for Mylar shows good qualitative agreement. Each curve has a pronounced maximum at the lowest coverage, followed by a minimum, a much smaller maximum, and a more shallow minimum. This periodic sequence disappears for higher coverages, where the system does not display the pronounced layering that occurs at lower coverages. A value of 0.005 for $\Delta\lambda$, the macroscopic inhomogeneity, gives good agreement for the overall scale. Given our relatively poor knowledge of the actual substrate potential, and the relatively simple way in which we have modeled the inhomogeneity, we take these results to indicate the qualitative correctness of the separation of the temperature width into homogeneous and inhomogeneous parts.

However, as mentioned earlier, Fig. 2 shows that the inhomogeneous width has half-layer periodicity, rather than the full-layer periodicity of the theoretical curves. In addition, the data shows cusplike behavior at minima that are essentially zero, whereas the theoretical minima are small but non-negligible relative to the maxima, and show no evidence of cusps.

V. SCENARIO FOR HALF-PERIODICITY AND CUSPS

We now discuss a scenario that, because half-periodicity, cusps, and true zeroes at the minima all occur at once, may be a possibility for explaining the data.

First, note that the "sensitivity" S (to the underlying substrate) should go to zero at high coverages, thus arguing for an envelope function that has this property [e.g., $\exp(-a\pi z)$, for some value of the parameter a]. Second, note that if S has the periodicity of the full layers and, through some unspecified mechanism, also changes sign

[e.g., $\sin(\pi z)$], the sensitivity then would have two zeroes per period. Since the value of S extracted from the data appears in the inhomogeneous width through its square [cf. Eq. (2)], the "experimental" value for S must be positive, and thus the zeroes of S must correspond to cusps. In Fig. 4 we plot an example consisting of the absolute value of $\sin(\pi z)\exp(-0.4\pi z)$; the exponential provides an envelope function that goes to zero at high coverages, and its coefficient was readily obtained by trial and error. Comparison with Fig. 2 shows a remarkable similarity, even in the way the curves are skewed toward lower coverages. Thus such a scenario can explain all three peculiar aspects of the data.

The key, then, is to find a mechanism that causes such a sign change in the sensitivity. A possibility that became available only well after the analysis and calculations for this work had been completed is contained in a more recent and more sophisticated version of the HNC theory. The improved theory includes "elementary diagrams." Moreover, the Jastrow-Feenberg wave function of (13) is improved by including three-body correlations $u_3(\mathbf{r}_i, \mathbf{r}_j, \mathbf{r}_k)$, which are determined by a three-body Euler equation corresponding to Eq. (14). This improved theory reproduces the bulk equation of state for ^{4}He, as well as the properties of ^{3}He-^{4}He mixtures to better than 0.1 K over a wide range of densities,[15] and leads to a significantly higher saturation density (0.0215 Å^{-3} compared with 0.017 Å^{-3} for the less sophisticated version employed above). In such a more "compact" system, hard-core effects are more pronounced. Preliminary results indicate that, when applied to the problem of films, the improved HNC theory leads to a sequence of phase transitions at half-filled layers.[16] These transitions occur when it becomes energetically favorable to elevate particles into the second layer rather than to further compress the first layer, and similarly for promotion into the second and the third layers (it is not yet clear how far this sequence will be seen, before layering no longer occurs). Thus, in addition to structure associated with the filling of each layer, there will be additional structure associated with the transfer of particles from one layer to the next. Each of these has the periodicity of the layers, but the first is associated with half-filling, and the second is associated with filling. In principle, then, there could be two independent mechanisms that, together, yield the observed half-periodicity. Whether this mechanism will be able to explain the observed features awaits the full development and application of the theory.

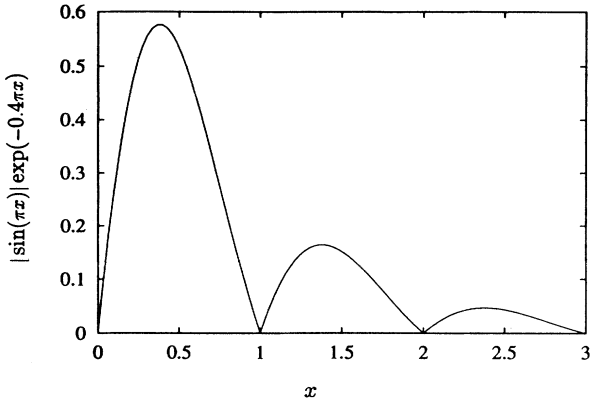

FIG. 4. $|\sin(\pi z)|\exp(-0.4\pi z)$, to be compared with Fig. 2.

ACKNOWLEDGMENTS

This work was supported in part by the National Science Foundation, Division of Materials Research (Low Temperature Program) under Grant No. DMR-8451893 (to G. A.) and under Contract Nos. PHY-8806265 and PHY-9108066 (to E. K.), and by the Texas Advanced Research Program under Grant Nos. 3046 and 10266-145 (to G. A.) and No. 10366-012 (to E. K.).

[1] P. C. Hohenberg, Phys. Rev. **158**, 383 (1967); N. D. Mermin and H. Wagner, Phys. Rev. Lett. **17**, 1133 (1966); N. D. Mermin, Phys. Rev. **176**, 250 (1968); D. Jasnow and M. E. Fisher, Phys. Rev. Lett. **23**, 286 (1969).
[2] J. M. Kosterlitz and D. J. Thouless, J. Phys. C **6**, 1181 (1973); J. M. Kosterlitz, *ibid.* **7**, 1046 (1974).
[3] D. R. Nelson and J. M. Kosterlitz, Phys. Rev. Lett. **39**, 1201 (1977).
[4] D. J. Bishop and J. D. Reppy, Phys. Rev. Lett. **40**, 1727 (1978); Phys. Rev. B **22**, 5171 (1980).
[5] P. W. Adams and W. I. Glaberson, Phys. Rev. B **35**, 4633 (1987).
[6] G. Agnolet, D. F. McQueeney, and J. D. Reppy, Phys. Rev. B **39**, 8934 (1988).
[7] V. Ambegaokar, B. I. Halperin, D. R. Nelson, and E. Siggia, Phys. Rev. B **21**, 1806 (1980).
[8] DuPont Company, Wilmington, DE.
[9] P. Minnhagen, Rev. Mod. Phys. **59**, 1001 (1987).
[10] D. F. McQueeny, G. Agnolet, G. K. S. Wong, and J. D. Reppy, Jpn. J. Appl. Phys. Suppl. 26-3 **26**, 79 (1987).
[11] D. F. McQueeney, Ph.D. thesis, Cornell University, 1988 (unpublished).
[12] J. Epstein and E. Krotscheck, Phys. Rev. B **37**, 1666 (1988).
[13] J. DuPont Roc (private communication).
[14] M. W. Cole and D. L. Goodstein, Rev. Mod. Phys. **53**, 199 (1981).
[15] E. Krotscheck, Phys. Rev. B **33** 3158 (1986); E. Krotscheck and M. Saarela, Phys. Rep. (to be published)
[16] B. E. Clements, E. Krotscheck, and H. J. Lauter (unpublished).